Journal of Cleaner Production 332 (2022) 130089

Contents lists available at ScienceDirect

Journal of Cleaner Production

journal homepage: www.elsevier.com/locate/jclepro

Use of screen glass and polishing sludge in waste-based expanded aggregates for resource-saving lightweight concrete

Sossio Fabio Graziano [a,*], Chiara Zanelli [b], Chiara Molinari [b], Bruno de Gennaro [c], Gaspare Giovinco [d], Cecilia Correggia [e,1], Piergiulio Cappelletti [e,f], Michele Dondi [b]

[a] Dipartimento di Farmacia, Università di Napoli Federico II, Via D. Montesano 49, 80131, Napoli, Italy
[b] CNR-ISTEC, via Granarolo 64, 48018, Faenza, Italy
[c] Dipartimento di Ingegneria Chimica, dei Materiali e della Produzione Industriale, Università di Napoli Federico II, Piazzale V, Tecchio 80, 80125, Napoli, Italy
[d] Dipartimento di Ingegneria Civile e Meccanica, Università di Cassino e del Lazio meridionale, viale dell'Università, 03043, Cassino, Italy
[e] Dipartimento di Scienze della Terra, dell'Ambiente e delle Risorse, Università di Napoli Federico II, via Vicinale Cupa Cintia 21, 80126, Napoli, Italy
[f] Centro Musei delle Scienze Naturali e Fisiche, Università di Napoli Federico II, via Mezzocannone 8, 80134, Napoli, Italy

ARTICLE INFO

Handling editor: Zhen Leng

Keywords:
Screen glass waste
Tile polishing mud
Lightweight expanded aggregate
Lightweight concrete
Industrial waste recycling

ABSTRACT

The purpose of this study is to evaluate different lightweight concretes for the first time formulated with lightweight expanded aggregates produced only with industrial waste. The motive is that a lack of knowledge still exists in the literature about how to integrate these waste-based aggregates in lightweight concrete. To achieve the desired bloating and aggregates physical properties, PC-TV screen glass and ceramic tile polishing sludge were selected as suitable raw materials. Both were characterized by mineralogical and chemical analyses and the effect of different combinations was pointed out. Hot-stage microscopy was used to determine the bloating rates and firing behavior. Lightweight expanded aggregates were obtained using both static laboratory kiln and rotating pilot kiln, by firing at maximum temperatures between 1150 and 1200 °C, to simulate the industrial production process and favor scaling up. The so obtained aggregates were characterized from the physical-mechanical point of view, highlighting an important bloating attitude and bulk density lower than 700 kg/m^3 for all the test conditions. Bulk density, water absorption and mechanical properties are fully comparable to commercial counterparts. The best material was used as coarse aggregate in lightweight structural concrete and cellular concrete prepared at pilot scale (for structural application and thermal/acoustic insulation, respectively). The technical properties are consistent with standard requirements of compressive strength (>25 MPa for lightweight structural concrete) and thermal conductivity (18–24 W/m*K for cellular concrete). These results demonstrate the technological feasibility of using waste-based aggregates into lightweight concrete design, according to a circular economy vision.

1. Introduction

The systematic switch-off of the analogical broadcasting system and the consequent passage to digital terrestrial broadcasting, is accompanied by huge replacement of old CRT (Cathode Ray Tube) apparels with new TV units equipped with LCD/LED screens (Hermans et al., 2001). Unfortunately, despite increasing efforts, few advances were made on the treatment process of e-wastes so that the preferred choice is still limited to landfilling (Baldé et al., 2017).

As reported by "The Global E-waste Monitor 2014: Quantities, flows and resources" (from the United Nations University), 41.8 million tons of electronic wastes and millions tons of cathode ray tube residues were produced in 2014 worldwide (Baldé et al., 2017). This trend is not expected to decrease in next years (Yao et al., 2018). The presence of hazardous elements, i.e. Pb in the tube and funnel glass and high amount of Sr and Ba in the screen glass (SG), generates problems related to old screens disposal and waste management (2000/532/ EC, 2000). The disposal of such component represents only among the various critical issues common to many other wastes from industrial activities that should be considered according to concepts of circular economy and reuse For this reason, several recent investigations (Behera et al., 2021; Camana et al., 2021; Chinnu et al., 2021; Lim et al., 2019; Liu and Coffman, 2016; Ma et al., 2021; Mpatani et al., 2021; Upadhyay et al.,

* Corresponding author.
E-mail address: sgraziano@unina.it (S.F. Graziano).
[1] Permanent address: D. Cimarosa st., 12–80029 Sant'Antimo (NA), Italy.

https://doi.org/10.1016/j.jclepro.2021.130089
Received 18 May 2021; Received in revised form 25 November 2021; Accepted 11 December 2021
Available online 14 December 2021

List of used abbreviations

C	Cellular concrete experimental specimen
CCAT	Charge Compensated Aluminium in Tetrahedral coordination
CRT	Cathode Ray Tube
DPM	Dried Polishing Mud
EDS	Energy Dispersive Spectroscopy
GNF	Glass Network Formers
GNM	Glass Network Modifiers
HSM	Hot Stage Microscope
LCD	Liquid Crystal Display
LEA	Lightweight Expanded Aggregates
LED	Light Emitting Diode
LS	Lightweight Structural concrete experimental specimen
LoI	Loss on Ignition
NBO/T	Non-Bridging Oxygens per Tetrahedrally-coordinated cations
SEM	Scanning Electron Microscope
SG	Screen Glass waste
SiC	Silicon Carbide
XRPD	X-Ray Powder Diffraction
XRF	X-Ray Fluorescence

2021; Wan et al., 2021) proposed a plenty of solutions aimed at using municipal or industrial wastes in the ceramic or building sectors, including Lightweight Expanded Aggregates (hereafter LEA) giving them a sort of second life as secondary raw materials (Dondi et al., 2009, 2016). This increased interest in LEA production is also boosted by a growing number of studies on the use of a wider range of urban and industrial wastes as materials for LEA production (Cáceres et al., 2019; Dondi et al., 2016).

According to standard definition, lightweight aggregates are mineral granular, with a bulk density not higher than 2000 kg/m^3 this latter considered as the key classifier parameter that distinguishes lightweight from dense aggregates (UNI EN 13055, 2016; Bush et al., 2006; de Gennaro et al., 2004). Lightweight aggregates have a lot of applications: e.g., as loose material, in back wall fillers and in the agronomic field or, once mixed with a binder, in the manufacture of plaster, asphalt and lightweight structural concrete, in particular in the production of thermo-acoustic insulators in lightweight concrete (Mindness et al., 2002). Due mainly to the increasing demand for lightweight structural and insulating (thermal and acoustic) mortars and concretes, LEA are currently the object of a revitalized interest (Kurpińska and Ferenc, 2020; Li et al., 2020; Oktay et al., 2015).

Artificial lightweight expanded aggregates are usually produced from natural raw materials (such as clay, shales or zeolites-rich rocks) able to bloat by themselves (Bush et al., 2006; de Gennaro et al., 2009; Dondi et al., 2016) through a quick heating at high temperature given by gases released during hating. If the ceramic matrix exhibits a suitable permeability and viscosity of the liquid phase, the formed gases can be then entrapped and the desired expansion is achieved (Molinari et al., 2020; Moreno-Maroto et al., 2020). If the ceramic matrix exhibits a suitable permeability and viscosity of the liquid phase, the formed gases can be then entrapped and the desired expansion is achieved (Molinari et al., 2020; Moreno-Maroto et al., 2020). When these conditions do not occur, the addition of an expanding agent is necessary. An industrial waste can be selected as gas-forming substance (Dondi et al., 2016). Dried Polishing Mud (hereafter DPM) from stoneware tile polishing process is known as bloating enhancer, given by silicon carbide contamination (about 1% SiC) derived by lapping tools abrasion (de Gennaro et al., 2007, 2009; Zanelli et al., 2021). At high temperature, SiC oxidises leading to dissociation and gas production (Molinari et al., 2021; Opila and Nguyen, 1998).

Overall, LEA are currently the object of a revitalized interest, due mainly to the increasing demand for lightweight structural and insulating (thermal and acoustic) mortars and concretes (Kurpińska and Ferenc, 2020; Li et al., 2020; Oktay et al., 2015; Xie et al., 2019).

This interest is also fueled by a growing awareness about environmental sustainability, which is stimulating various studies on the use of urban and industrial wastes as possible raw materials for LEA production (Amin et al., 2020; Cáceres et al., 2019; Dondi et al., 2016).

Such new generation of raw materials is often characterized by a much wider range of chemical and mineralogical composition with respect to clays and shales. For this reason, this new kind of aggregates often shows a different technological behavior, imposing some adjustments to the manufacturing process (shaping and firing treatments) in order to meet the expected product specifications.

Glass-based batches represent a test-bench of chemical composition and operative conditions, in order to appraise the role of the physical properties of LEA in binder hardening, such as water absorption, bulk density, and mechanical strength. Another goal is to go further the state of the art for waste recycling: in literature there is a certain number of papers dealing with expansion of waste glass (Adhikary et al., 2021; Bernardo et al., 2010; Ducman et al., 2002; Kourti and Cheeseman, 2010; Li et al., in press; Molinari et al., 2021; Mueller et al., 2008; Pascual et al., 2021; Tuan et al., 2013; Wei et al., 2011; Yio et al., 2021) but no one exist, at best of our knowledge, using glass waste from PC and TV screen and moreover on concretes based on these LEA.

Unlike other papers, this research:

- aims to demonstrate the technological feasibility of different lightweight concretes for the first time formulated with waste-based aggregates;
- Evaluates the full production chain: from the formulation of suitable LEA batches by utilizing only waste (PC-TV screen and SiC-containing porcelain stoneware tile polishing sludge), to the upscaling of LEA manufacturing to a pilot line, to eventually formulate, produce and characterize the lightweight concretes containing waste-based LEA.

The paper is so structured: after the description of experimental activities (section 2), the results are illustrated and discussed, first about waste characterization and mix formulation (section 3.1) then moving to LEA production and characterization (section 3.2) and finally production and characterization of lightweight concretes (section 3.3).

2. Materials and methods

Two wastes were selected from same number Italian waste management facilities: a glass from TV-PC screen (SG) and a mud from the polishing of ceramic tiles (DPM). Both starting materials and fired products were characterized by:

2.1. Mineralogical composition

Mineralogical qualitative and quantitative analysis (Table 1) were performed by X-ray powder diffraction (XRPD) using a Panalytical X'Pert Pro diffractometer, equipped with a RTMS X'Celerator detector with Cu-Kα radiation, operating at 40 kV and 40 mA. Scans were collected in the range 5–80 °2θ using a step interval of 0.017 °2θ, with a step counting time of 120 s. Mineral phases were identified by the Panalytical Highscore Plus 3.0c software and PDF-2/ICSD mineral databases and quantitative phase Rietveld refinement were performed using Topas software (version 5.0, Bruker, Germany) (Bish and Howard, 1988; Bish and Post, 1993; Rietveld, 1969). Crystalline and vitreous phases were calculated by means of internal standard method (20 wt% of Al_2O_3, 1 μm, Buehler Micropolish).

Table 1
Chemical and mineralogical composition of waste and their characteristic temperatures by hot-stage microscopy. [a]Expansion <100 vol% is assumed for samples that did not reach the initial volume after the first sintering phase.

Components	Units	Ceramic tile polishing sludge (DPM)	TV and PC screen glass waste (SG)
SiO_2	wt%	66.37	63.78
TiO_2		0.55	0.41
Al_2O_3		19.35	2.34
Fe_2O_3		0.81	0.10
MgO		2.64	0.31
CaO		1.64	1.02
SrO		0.05	7.73
BaO		0.04	8.55
Na_2O		3.47	7.53
K_2O		1.81	7.22
P_2O_5		0.26	–
Loss on ignition		3.00	1.02
Quartz	wt%	18	2
K-feldspar		3	–
Plagioclase		3	–
Vitreous phase		72	98
Others (mullite, zircon, SiC, etc.)		3	tr
Sintering temperature (T_s)	°C	1185 ± 5	695
Softening temperature (T_r)	°C	1220 ± 5	855
Melting temperature (T_f)	°C	1330 ± 5	1080
Temperature of maximum expansion (T_{me})	°C	1240 ± 5	1215
Temperature of max expansion rate (T_{mve})	°C	1220 ± 5	1200
Maximum volume expansion at T_{me}	vol%	310 ± 0.1	<100[a]
Isothermal expansion after 30 min at T_{mve}	vol%	250 ± 0.1	<100[a]

2.2. Chemical composition

Chemical analyses of raw materials were carried out, on pressed powder pellets, using an Axios Panalytical X-ray fluorescence (XRF) spectrometer, equipped with six analyzer crystals, three primary collimators and two detectors (flow counter and scintillator). Analytical uncertainties are 1–2% for major elements and 5–10% for trace elements (Cucciniello et al., 2017). The weight Loss on Ignition (LoI) was determined by gravimetric techniques, firing at 1000 °C powders previously dried at 110 °C overnight.

2.3. Firing behavior and LEA production

Firing behavior was evaluated by a Hot-Stage Microscope (HSM - Expert System Solutions - Misura 2) on cylindrical specimen heated with a heating rate of 10 °C/min until melting (2 mm diameter, 3 mm height) (Dondi et al., 2001). The laboratory scale batches were designed with the goal of maximizing the amount of wastes that allow to comply with the required physical and technological properties of the products. The mix design and the obtained chemistry are reported in Table 2. Laboratory simulation of LEA manufacturing process was conducted on three mixes by preparing about 8 g of powder and pressing at 40 MPa (pellets with a diameter of 10 mm). The pellets were fired in electric chamber static kiln (Nannetti mod. CV) at maximum temperatures of 1150 and 1200 °C and 5 min well time. Moreover, the best mixture of was chosen to a larger scale production (35 L) and in rotating inclined kiln (Lab scale prototype from Nannetti) for about 40 min, with 5 min of soaking time and at the maximum temperature of (1225 °C) (de Gennaro et al., 2009).

2.4. Composition and properties of the vitreous phase

Based on bulk chemistry and mineralogical properties of the fired bodies, chemical composition of vitreous phase was determined to evaluate glass structure parameters (Table 3). The chemical composition of the vitreous phase was calculated by subtracting from the bulk chemistry of the fired body the contribution of mineralogical phases, assuming their stoichiometric compositions weighted on the quantitative phase analysis. Physical properties at high temperature were estimated by predictive models based on the chemical composition of the liquid phase (Fluegel, 2007). The vitreous phase contains different elements that affect both structure and properties of the glass network. In order to facilitate data interpretation, some parameters were used to express specific structural features of the melt:

Table 2
Mix design and chemical composition of the LEA batches.

Mix design (wt %)	Mix 1	Mix 2	Mix 3
DPM	40	50	60
SG	60	50	40
Chemical composition of the LEA batches (wt%)			
SiO_2	66.03	66.43	66.83
TiO_2	0.47	0.49	0.50
Al_2O_3	9.40	11.16	12.92
Fe_2O_3	0.40	0.47	0.54
MgO	1.27	1.51	1.75
CaO	1.29	1.36	1.42
SrO	4.71	3.93	3.16
BaO	5.20	4.34	3.48
Na_2O	5.99	5.59	5.19
K_2O	5.12	4.58	4.04
P_2O_5	0.11	0.13	0.16
Loss on Ignition	1.80	2.00	2.21

Table 3
Phase composition together with the chemical composition and estimated shear viscosity of the vitreous phase.

Samples	Mix1		Mix2		Mix3	
Firing temperature (°C)	1150	1200	1150	1200	1150	1200
Bulk density (kg/m^3)	710	770	740	730	740	770
Phase composition (wt%)						
Quartz	2	1	2	3	3	3
K-feldspar	9	8	12	10	18	14
Plagioclase	5	5	5	5	2	2
Vitreous phase	84	86	81	82	77	81
Chemical composition of the vitreous phase (wt%)						
SiO_2	65.52	65.91	66.04	65.59	66.11	66.04
TiO_2	0.56	0.55	0.60	0.60	0.65	0.62
Al_2O_3	7.86	7.89	9.64	9.97	11.90	12.22
Fe_2O_3	0.48	0.47	0.58	0.57	0.70	0.67
BaO	6.19	6.05	5.36	5.29	4.52	4.30
SrO	5.61	5.48	4.85	4.79	4.10	3.90
MgO	1.51	1.48	1.86	1.84	2.27	2.16
CaO	1.28	1.25	1.42	1.40	1.73	1.65
Na_2O	6.58	6.42	6.32	6.25	6.50	6.18
K_2O	4.28	4.38	3.15	3.52	1.30	2.07
P_2O_5	0.13	0.13	0.16	0.16	0.21	0.20
NBO/T[a] (1)	0.26	0.26	0.25	0.25	0.23	0.23
GNF[b] (% atom)	34.79	34.98	35.98	35.94	37.20	37.33
CCAT[c] (% atom)	4.16	4.18	5.10	5.28	6.30	6.47
GNM[d] (% atom)	18.21	17.85	15.38	15.29	12.33	11.95
Viscosity (Log_{10} Pa s)	3.04	2.77	3.30	2.98	3.55	3.24

[a] (NBO/T) Degree of polymerization of the melt - From the composition of the liquid phase: Number of Non-Bridging Oxygens (NBO) per Tetrahedrally-coordinated cations (Si,Al) as atomic percentage.

[b] (GNF) Glass network formers - From the composition of the liquid phase: GNF (atom%) = Si + CCAT, corresponding to Al^{3+}charge compensated by alkali or alkaline earths.

[c] (CCAT) Charge compensated aluminium in tetrahedral coordination - From the composition of the liquid phase: Al^{3+} charge compensated by alkali and alkaline earths: CCAT(atom%) = Na + K+2Ca+2 Mg (up to max value = Al).

[d] (GNM) Glass network modifiers - From the composition of the liquid phase: alkali and alkaline earths exceeding CCAT: GNM (atom%) = Na + K+2 Mg+2Ca–CCAT.

- Degree of depolymerization of the melt (NBO/T) defined as the number of Non-Bridging Oxygens (NBO) per tetrahedrally-coordinated cations (Si, Al) as atomic percentage and calculated from the composition of the vitreous phase;
- Glass network formers (GNF) - From the composition of the liquid phase: GNF (atom%) = Si + CCAT, corresponding to Al^{3+} charge compensated by alkali or alkaline earths.
- Charge compensated aluminium in tetrahedral coordination (CCAT) - From the composition of the liquid phase: Al^{3+} charge compensated by alkali and alkaline earths: CCAT(atom%) = Na + K+2Ca+2 Mg (up to max value = Al).
- Glass network modifiers (GNM) - From the composition of the liquid phase: alkali and alkaline earths exceeding CCAT: GNM (atom%) = Na + K+2 Mg+2Ca–CCAT.

2.5. Microstructure

Micro-textural observations were carried out by Scanning Electron Microscopy coupled with Energy Dispersive Spectroscopy (SEM-EDS; JEOL JSM-5310 coupled with Oxford Instruments Microanalysis Unit equipped with an INCA X-act detector) and by using the digital microscope (HIROX RH-2000).

2.6. LEA and concrete characterization

Physical and technological properties of LEA were tested by means of European Standards: bulk density (kg/m^3) (Archimede's principle), loose bulk density (kg/m^3), strength of particle (MPa) (Control Test equipment - load rate 1 MPa*s-1, 20 samples), particle size distribution (mm) and water absorption (%) (UNI EN 13055, 2016). As regards concretes, four different batches were designed and produced following standard indications (UNI 11013, 2002) in order to test LEA-containing concretes and regular ones (as reference) for each feature. For this reason, two kind of lightweight structural concretes (LS1-LS2) and cellular concretes (C1–C2) were cured in a controlled temperature chamber (20 °C for three days) then in water filled tanks (20 °C) until final maturation (28 days) (UNI EN 12390-1, 2012; UNI EN 12390-2, 2019).

Lightweight structural concretes were tested by means of mass volume and compressive strength, on cubic specimens (15 × 15 × 15 cm) (UNI EN 12390-3, 2019; UNI EN 12390-4, 2019; UNI EN 12390-7, 2021).

Cellular concretes were tested by means of mass volume (UNI EN 12390-7, 2021) and thermal conductivity, on tile shaped specimens (20 × 20 × 3 cm). Thermal conductivity evaluation followed experimental procedures reported in literature (Buonanno et al., 2003; Dell'Isola et al., 2012; Frattolillo et al., 2005; ISO/IEC Guide 98-1, 2009). The latter based on a one-dimensional steady state comparative method and expanded uncertainty with a level of confidence of 95%. In particular, a temperature gradient is established across the sample using electrical heaters and a thermostatic bath. The sample is bounded above and below by two reference structures, each comprising a glass plate between two isothermal copper parallel plates. Under the hypothesis of one-dimensional (vertical) heat flux and negligible boundary thermal losses, the effective thermal conductivity (λ) can be evaluated as the arithmetic mean of the thermal conductivity values obtained by equating the heat fluxes measured at the top, middle and at the bottom of the sample. That is, the heat flow through the sample can be measured by measuring the temperature gradient across reference Pyrex® glass plates, whose thermal conductivity and its corresponding uncertainty is known.

3. Results and discussion

3.1. Waste characterization and mix formulation

Both wastes were selected with a particle size distribution of less than 200 μm, which falls within the general trends identified to obtain the best behavior in terms of both expansion and technological properties of LEA (Dondi et al., 2016).

Both ceramic sludge and screen glass have a high silica content (about 65%), in accordance with literature data (Méar et al., 2006) and about 23% of fluxing content (i.e., the sum of Fe_2O_3+CaO + MgO + Na_2O + K_2O + SrO + BaO). The ceramic tile polishing sludge (DPM) has a composition close to the porcelain stoneware, being mainly constituted by glassy phase plus crystalline components like quartz, plagioclase and minor quantity of mullite, zircon and synthetic silicon carbide (Table 1).

SG waste is characterized by high amounts of SrO and BaO (~8 wt %), confirming the not-recycling attitude of this waste according to European Directives (2000/532/ EC, 2000, 2001/118 /EC, 2001, 2001/119 /EC, 2001, 2001/573/ EC, 2001, 2014/ 955/EU, 2014) and indirectly the need to provide alternatives to landfill disposal. The only crystalline phase present is a 2 wt% of quartz, probably due to a contamination during recycling operations (Table 1).

The thermal behavior of the two wastes is completely different: the glass sample exhibits characteristic temperatures much lower than those of DPM with no evident expansion (Table 1). In contrast, DPM exhibits an isothermal expansion of 310% after firing. On the basis of this peculiar behavior, the only way to use the SG waste is to mix it with DPM, known to play a bloating-enhancer role (de Gennaro et al., 2007, 2009; Monteiro et al., 2004). Formulation and composition of the selected mixtures are reported in Table 2.

3.2. LEA production and characterization

Firing conditions were set to be consistent with previous experimental researches (de Gennaro et al., 2007, 2009) and following suggested temperatures from Hot Stage Microscope (HSM) results.

Bulk density values were evaluated for samples fired at 1150 and 1200 °C (Fig. 1) with 5 min of well time and are reported in Table 3. All samples show bulk density values below 1000 kg/m^3 and, in particular, sample Mix1 has the lowest density value (710 kg/m^3) after firing at 1150 °C.

The mineralogical composition of waste-based LEA consists in K-feldspar, plagioclase, quartz, and abundant vitreous phase. (Table 3). Changes of the mineralogical composition of the bodies is mirrored in the chemical composition of the vitreous phase which in turn determines the degree of polymerization and physical properties, like shear viscosity at high temperature (Table 3). It is known that for a vitreous phase content higher than 75 wt%, both bulk viscosity and bloating index are mainly controlled by the chemical composition of the vitreous phase (Kaz'mina, 2010). In this study, the vitreous phase is always higher than 75% (77–86 wt%) therefore, the effect of bloating index, in relation to the chemical composition of the vitreous phase and its physical properties, was investigated (Table 3). Growing the percentage of DPM waste (both at 1150 and 1200 °C) the contents of SiO_2, Al_2O_3, TiO_2, Fe_2O_3, MgO increased in the vitreous phase, while the amounts of Na_2O, K_2O, BaO and SrO decreased.

The progressive increase of DPM brought about a gradual shift in the structural features of the melt, which turned slightly more polymerized (Number of Non-Bridging Oxygens per Tetrahedrally-coordinated cations (Si,Al) as atomic percentage NBO/T passing from 0.26 to 0.23). This

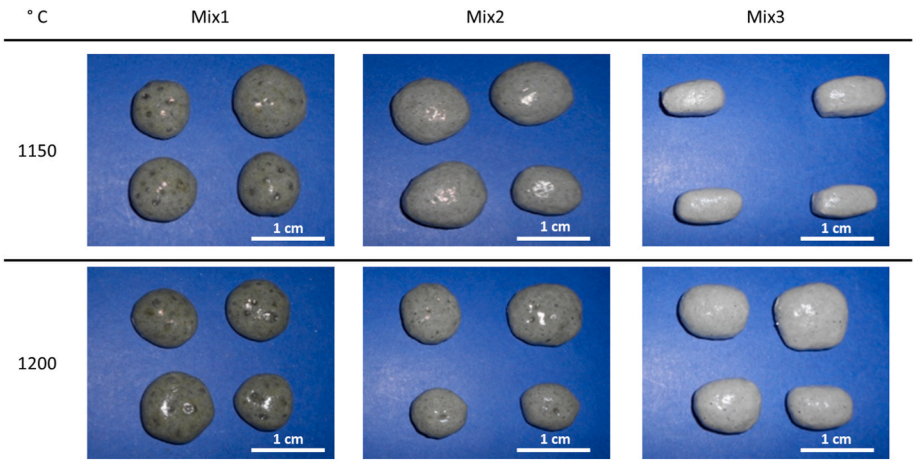

Fig. 1. Appearance of LEA fired at 1150 °C and 1200 °C.

trend agrees with the strong decrease of glass network formers and the growth of network formers (Table 3). This latter is mainly due to the incorporation of tetrahedrally-coordinated aluminum in the network charge compensated by alkali.

Such a chemical composition of the liquid phase reflects in a decreasing fluidity at high temperature, as suggested by the increase of viscosity with the increase of the DPM content.

As reported in literature (Petersen et al., 2017), the viscosity window for obtaining a low-density glass foam, observed for bottle glass with SiC as foaming agent, is between 3.3 and 4.0 $\log_{10}$ Pa s range, that can be compared with the values calculated for the studied mixtures. In particular, these values correspond to the viscosity data calculated for these bodies (Mix1, 2, 3). At firing temperature of 1150 °C, the sample Mix1 is the less dense (710 kg/m^3) with a viscosity value of 3.04 $\log_{10}$ Pa s. Temperature rising reduces glass viscosity, both favoring SiC oxidation and allowing gas expansion and bloating. At the same time, progressive decrease of glass viscosity favors bubbles coalescence and gas leaching, so reducing expansion efficiency and leading to higher bulk density (Molinari et al., 2020; Wang et al., 2018).

The presence of solid particles boosts the effective viscosity of the glass-crystals system (Giordano, 2019; Giordano et al., 2008; Prousse-vitch et al., 1993). At the same time, foam stability and bloating efficiency are limited (Dondi et al., 2016). Given the presence of the same crystalline structures in similar amounts, it is believed that the effect of the solid load is the same and therefore can be overlooked. Based on the main physical and chemical properties discussed, all the tested mixes are suitable for the use as coarse aggregate in concrete manufacturing (Molinari et al., 2020; Wang et al., 2018).

However, Mix1 was chosen for the pilot scale production (35 L – Mix1L) as the best compromise between the largest amount of waste glass used in mix design and good LEA technical features (firing temperature = 1150 °C; particles density = 710 kg/m^3). LEA produced with the rotary kiln have a glassy but rough external surface (Fig. 2a) which reasonably will favor the adherence between aggregate and cement.

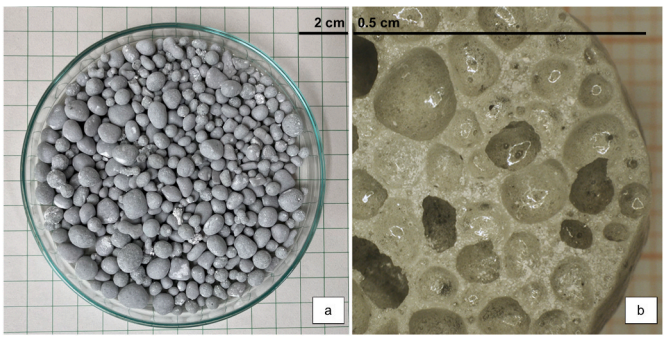

Fig. 2. Appearance of large-scale LEA production fired at 1150 °C.

Proceeding with a refining process for operative conditions for a large-scale production, thermal behavior of Mix1L was tested and results are reported in Table 4. Indeed, based on T_{mve} (1125 °C) and considering the gap between the inner part of the rotary tube and the value detected by the thermocouple (external to rotating tube) of the oven, a production temperature of 1225 °C was chosen (de Gennaro et al., 2009). By the technical viewpoint, Mix1L aggregates have similar mineralogical composition and viscosity, once compared to the samples prepared at the small laboratory scale (Mix 1 LEA), keeping close to the viscosity window for obtaining a low-density glass foam reported in literature (Petersen et al., 2017).

In the Mix1L, also the microstructure was evaluated in terms of quantity and quality of both pores and septa constituting the expanded structure (Figs. 2b and 3). Micrographs show that bubbles produced by bloating are characterized by a bimodal size distribution: a first population, with bubble diameters ranging from 100 to 500 μm (Fig. 3a) and

Table 4
Phase composition of Mix1L (large-scale production in rotary kiln at 1225 °C). Chemical composition and viscosity of the vitreous phase. Characteristic temperatures of LEA evaluated by hot stage microscope (HSM).

Phase composition (wt%)	Unit	Mix1L
Quartz	wt%	2
K-Feldspar		7
Plagioclase		3
Vitreous phase		88
Chemical composition of the vitreous phase (wt%)		
SiO_2	wt%	64.52
TiO_2		0.60
Al_2O_3		7.40
Fe_2O_3		0.51
MgO		1.63
CaO		1.17
SrO		6.04
BaO		6.67
Na_2O		6.60
K_2O		4.72
P_2O_5		0.14
Viscosity	(Log_{10} Pa s)	2.97
Sintering temperature (T_s)	°C	1010
Softening temperature (T_r)	°C	1018
Melting temperature (T_f)	°C	1323
Temperature of maximum expansion (T_{me})	°C	1233
Temperature of max expansion rate (T_{mve})	°C	1125
Maximum volume expansion at T_{mve}	%	220
Isothermal expansion after 30 min at the T_{mve}	%	160

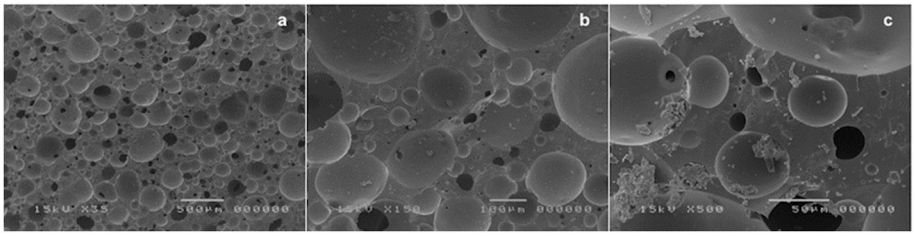

Fig. 3. Micrographs of the internal microstructure of the Mix1L aggregates in section: the scale bar is 500 μm (a), 100 μm (b) and 50 μm (c).

a class of smaller bubbles, ranging from 10 to 50 μm, mainly present in walls (septa) between larger bubbles (Fig. 3c) as already reported for this type of LEA (de Gennaro et al., 2009).

The physico-mechanical features of experimentally produced LEA were evaluated according to standard procedure (UNI EN 13055, 2016) and compared to those of some commercial products with a similar bulk density value (Table 5). As commercial products, in general, also waste-based LEA offer, as whole, a remarkable range of physical characteristics (e.g., bulk density and water absorption) and processing conditions (e.g. firing behavior). Leaching tests were performed in previous investigations on ceramic materials containing PC-TV glass (Raimondo et al., 2007; Dondi et al., 2009) or polishing sludge (García-Ten et al., 2016; Sarani et al., 2018). No mobilization of elements of concern (Ba, Sr, transition metals) was observed in vitrified products (Raimondo et al., 2007; García-Ten et al., 2016) at variance of the few mg/kg of Ba and Sr found in leachates from porous products (Dondi et al., 2009; Sarani et al., 2018).

3.3. LEA in lightweight concretes

Mix-designing concrete composition must start from an initial prevision of required concrete performances (workability, mechanical resistance, durability, etc.) and from the characteristics of the available raw materials (cement, aggregates, additives). According to this consideration, mix-design is based on some experimental correlations between the composition of the concrete, on one hand, and the performance of the hardened concrete by means of the characteristics of the used materials, on the other (Collepardi et al., 2016; Lydon, 1972; Neville, 2012).

Briefly summarizing the fundamental experimental correlations among components, is possible to assume that:

1 The water amount (in kg/m^3) influences the workability of the fresh mix (and hardened concrete performances) and can depend by the type of aggregate (rounded or crushed), its size (maximum diameter) and presence of additives (water reducers and aerating agents).
2 The water/cement ratio (w/c) represents the relationship between the total amount of water in the mix by weight, including the humidity of the aggregates, and the amount of cement. It is a fundamental parameter for the quality of concrete, capable of influencing numerous important characteristics and performances such as mechanical strength of the hardened conglomerate, permeability, the extent of shrinkage, etc. The optimal w/c value to produce a hardened concrete with high compressive strength and low permeability is 0.4 (Collepardi et al., 2016; Lydon, 1972; Neville, 2012)
3 The volume of inert material is calculated by difference through a balance of volume by subtracting from the volume of concrete, those of the other ingredients (i.e., the volumes of water, cement and air);
4 Volume of the total aggregate amount is divided by contributions of two main classes of aggregates (commonly sand and gravel) based on the granulometric curves with respect to the optimal curve chosen (Fuller, Bolomey, Cubic).

From the above reported consideration the role of water amount is a key for a correct mix-design and a very important contribution is due water absorption of aggregates. In fact, while an unsaturated aggregate removes water from the mixture, one with a wet surface provides water

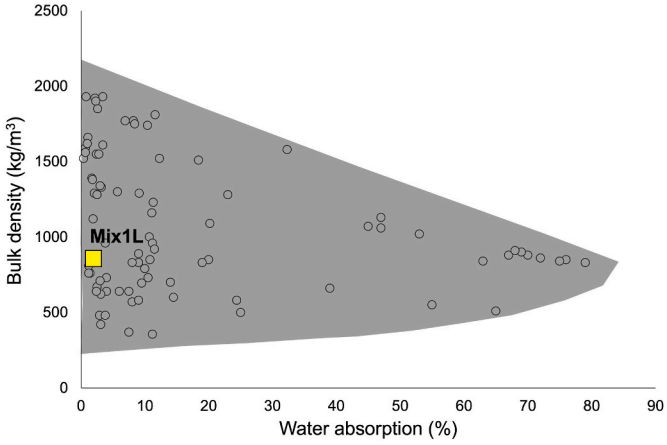

Fig. 4. Bulk density of LWA from waste as a function of water absorption (Dondi et al., 2016).

Table 5
Physical-mechanical features of waste-based aggregates compared to those of some commercial products with a similar bulk density value.

	Sample	Particle size distribution (mm)	Bulk density (kg/m^3)	Loose bulk density (kg/m^3)	Water absorption (24h) (%)	Strength of particle (MPa)
commercial LEA	Knauf[a]	3–8	<1000	440 (±15%)	<13	<2
	Granulati Zandobbio[b]	3–8	<1000	450 (±15%)	>10	>1
	Termolite[c]	3–8	<1000	380 (±15%)	>10	>1
	Leca[d]	3–8	<1000	380 (±15%)	>10	>1
	Leca più[d]	3–8	<1000	380 (±15%)	<10	>1,5
	Mix1L	3–10	860	670	2.05	1.54

[a] www.knauf.it.
[b] www.granulati.it.
[c] www.termolite.info.
[d] www.leca.it.

to the mixture. In order to respect a w/c ratio close to the optimal value (0.4), the use of an aggregate giving small water absorption coefficient is encouraged (Collepardi et al., 2016; Lydon, 1972; Neville, 2012).

Comparing technical features achieved on Mix1L, with literature data (Fig. 4), waste-based aggregates fall within the field of materials with low density and low water absorption (Dondi et al., 2016). The latter feature is due to the glassy surface created during firing.

Aggregate size plays another key role to produce a concrete with the maximum possible density, or with the lowest number of voids between individual granules. The particle size curve of the solid system (cement + aggregate) must follow specific equations that guarantee the maximum dimensional sorting and the right compromise between density and workability (Fennis and Walraven, 2012).

If large size aggregates are in excess, the mixture would be hardly workable without the addition of water (that can be considered detrimental to mechanical characteristics) on the contrary, if fine aggregate is in excess, a greater amount of water is required to wet the entire surface, determining, again, a high water/cement ratio. For this reason, three particle size distribution curves were commonly used to have the best particle size distribution: the Fuller curve, the Bolomey curve and the Cubic curve (Collepardi et al., 2016). As clearly visible in Fig. 5, Mix1L lot, was sieved and selected to be consistent with Fuller curve trend for an optimal particle size packing.

To test the possible use of Mix1L aggregate in concrete manufacturing, two different types of batches were prepared following common experimental recipes and using mix design reported in Table 6:

1) Lightweight Structural concretes (LS specimens).
2) Foamed Cellular concretes (C specimens).

The lightweight structural concrete is useful to build elevations of existing buildings that are not strong enough to bear the weight of ordinary concrete structures and which would therefore require complex adaptation interventions to increase their bearing capacity. The use of a structural lightweight concrete reduces, also, the inertia forces that arise when the structure is subject to seismic movements, allowing a decrease in the reinforcement with the same section, or a decrease in the resistant section with the same reinforcement (Collepardi et al., 2016; Neville, 2012).

The foamed cellular concrete, instead, is produced by mixing, in a foaming equipment, a cement grout with a protein-based foam obtained with specific foaming agents. In this way, a closed air cell structure coated with cement is formed inside the cement mixture, giving high insulating power and considerable lightness to the material.

As regards "LS", mix design were experimentally conceptualized with two different ratios (LS1 and LS2) between fine and coarse aggregates (to better estimate waste-based aggregates contribution to concrete properties), both with the same w/c ratio (0.46). For "C" mix design, a common recipe without coarse aggregate addition was considered (C1 - reference) along with a waste-based aggregates addition recipe (C2) for a direct comparison.

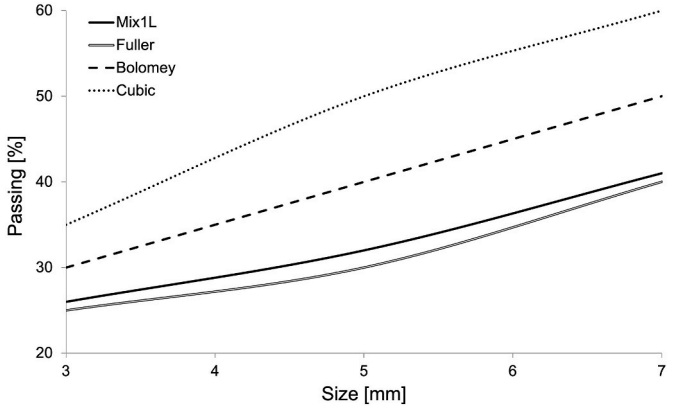

Fig. 5. Particle size distribution of Mix1L.

Accordingly, to their final application, the two types of concrete, containing experimental Mix1L aggregates, have been tested for compressive strength (LS specimens) and thermal conductivity (C specimens) (Table 6). Standard values are reported for reference (UNI EN 1745, 2020; UNI EN 206, 2016). Standard values of thermal conductivity for C2 sample have to be intended as cross-class concrete value between "aerated concrete units" and "other aggregates concrete unit" as reported in standard (UNI EN 1745, 2020).

By experimental results analysis (Table 6) is evident that LS1 and LS2 concretes show typical features of lightweight structural concretes as indicated by standard definition (UNI EN 206, 2016) and in literature (Pacenti, 1980) (Mass volume between 1400 and 2000 kg/m^3 and compressive strength, for structural purposes, substantially higher than 20 MPa).

Thermal insulation represents the main field of application for cellular concretes, for this reason is very important to achieve values of thermal conductivity similar to those of commonly used foamed concretes, usually these values range from about 0.14 to 0.24 W/(m K) (Bumanis et al., 2013; UNI EN 1745, 2020), lower is the value better is the insulation.

From comparison between C1 (assumed as reference) and C2 is possible to notice that experimental specimen (C2) seems to improve the insulating properties of a "regular" foamed concrete (C1) showing a measured thermal conductivity value of 0.18 W/(m K).

Comparing experimental results with literature data (Samson et al., 2017) (along with references therein) (Fig. 6 a,b) is clearly visible that innovative concretes produced in this work and containing waste-based aggregates can be considered as trend-followers of other, commercial or not, products.

4. Conclusions

A proof-of-concept of lightweight concrete manufacturing by using waste-based lightweight aggregates was demonstrated all along the production chain.

As a case that has received less attention, we tested possibility to go further the state of the art for glass waste recycling, using this secondary raw material in LEA-based concretes.

Novelty of this work can be summarized as follows:

- PC-TV screen waste glass and ceramic polishing sludge are suitable secondary raw materials to achieve the desired bloating under industrial production conditions. An optimal ratio was found as a compromise between the 40 wt% of ceramic tile polishing sludge and TV and the 60 wt% of PC screen glass waste.
- The selected formulation allows to produce LEA with physical and mechanical properties fully comparable with commercial aggregates. This paves the way to bending the LEA supply chain towards a circular array by replacing to a large extent ordinary expanded clay with waste-based aggregates.
- Both lightweight structural and cellular concretes manufactured with waste-based LEA exhibit a technological behavior fully complying with the performances required by regulations in the building sector.

The achieved results disclose interesting opportunities for waste application in LEA production and related lightweight concrete formulation, rising the circular economy quote in the building sector. This possibility becomes even more appealing considering the growing demand for sustainable building products.

Next steps will be focused on both the life cycle assessment of the waste-based LEA production and the evaluation of hazardous elements stabilization. Further improvements concern a widening of the waste

Table 6
Batch formulation and physical features of concretes. Std val: standard values [a](UNI EN 206, 2016), [b](UNI EN 1745, 2020).

Properties	Unit	Lightweight Structural			Cellular		
		LS1	LS2		C1	C2	
Portland 42.5R	kg/m^3	350	350		300	300	
Sand (0–4 mm)	kg/m^3	833	500		600	600	
LEA (Mix1L)	L/m^3	400	550		–	–	
	L	–	–		–	440	
W/C ratio	1	0.46	0.46		0.66	0.66	
Additive Sika ViscoCrete-5380	L/m^3	4.55	4.55		–	–	
Additive CaO dry	kg/m^3	–	–		6	6	
Foaming additive	kg/m^3	–	–		37	37	
Water	L	161	161		200	200	
				Std val[a]			Std val[b]
Mass volume (density-curing time 28 days)	kg/m^3	1800.5 ± 10	1661.5 ± 12	1400 < D < 2000	1082.6 ± 5	1007.7 ± 6	800 < D < 1400
Compressive strength	MPa	26.6 ± 1	25.2 ± 1	R_{ck} >20	–	–	
Thermal conductivity and expanded uncertainty with a 95% level of confidence	W/m·K	–	–		0.24 ± 0.05	0.18 ± 0.03	0.14–0.24

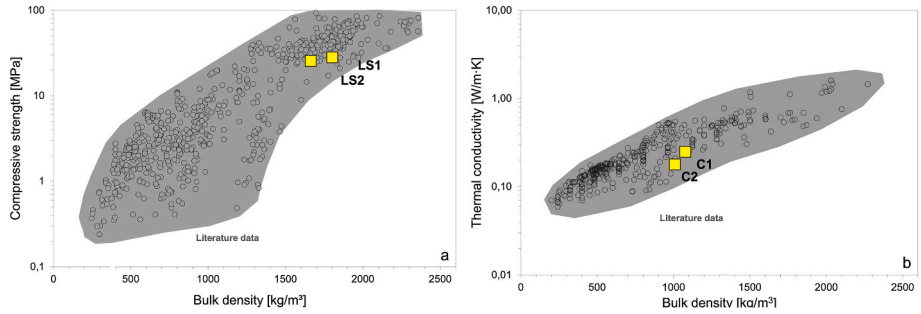

Fig. 6. Compressive strength (a) and thermal conductivity (b) as a function of bulk density for lightweight concretes containing different kind of aggregates. (data after Samson et al., 2017).

compositional range and solutions to lower the firing temperature to approach that applied in the manufacturing of expanded clay.

CRediT authorship contribution statement

Sossio Fabio Graziano: Conceptualization, Methodology, Formal analysis, Investigation, Writing – original draft, Writing – review & editing. **Chiara Zanelli:** Methodology, Formal analysis, Investigation, Writing – review & editing. **Chiara Molinari:** Formal analysis, Investigation, Writing – review & editing. **Bruno de Gennaro:** Conceptualization. **Gaspare Giovinco:** Methodology, Formal analysis, Investigation. **Cecilia Correggia:** Methodology, Formal analysis, Investigation. **Piergiulio Cappelletti:** Conceptualization, Supervision, Writing – review & editing. **Michele Dondi:** Conceptualization, Supervision, Writing – review & editing.

Declaration of competing interest

The authors declare that they have no known competing financial interests or personal relationships that could have appeared to influence the work reported in this paper.

References

2000/532/EC, 2000. European Commission Decision of 3 May 2000 Replacing Decision 94/3/EC Establishing a List of Wastes Pursuant to Article 1(a) of Council Directive 75/442/EEC on Waste and Council Decision 94/904/EC Establishing a List of Hazardous Waste.
2001/118/EC, 2001. European Commission Decision of 16 January 2001 Amending Decision 2000/532/EC as Regards the List of Wastes.
2001/119/EC, 2001. European Commission Decision of 22 January 2001 Amending Decision 2000/532/EC Replacing Decision 94/3/EC Establishing a List of Wastes Pursuant to Article 1(a) of Council Directive 75/442/EEC on Waste and Council Decision 94/904/EC.
2001/573/EC, 2001. European Council Decision of 23 July 2001 Amending Commission Decision 2000/532/EC as Regards the List of Wastes.
2014/955/EU, 2014. European Commission Decision of 18 December 2014 Amending Decision 2000/532/EC on the List of Waste Pursuant to Directive 2008/98/EC of the European Parliament and of the Council.
Adhikary, S.K., Ashish, D.K., Rudžionis, Ž., 2021. Expanded glass as light-weight aggregate in concrete – a review. J. Clean. Prod. https://doi.org/10.1016/j.jclepro.2021.127848.
Amin, M., Tayeh, B.A., Agwa, I.S., 2020. Effect of using mineral admixtures and ceramic wastes as coarse aggregates on properties of ultrahigh-performance concrete. J. Clean. Prod. 273. https://doi.org/10.1016/j.jclepro.2020.123073.
Baldé, C.P., Forti, V., Gray, V., Kuehr, R., Stegmann, P., 2017. The Global E-Waste Monitor 2014 : Quantities, Flows and Resources. United Nations University, IAS Scycle, Bonn, Germany.
Behera, M., Nayak, J., Banerjee, S., Chakrabortty, S., Tripathy, S.K., 2021. A review on the treatment of textile industry waste effluents towards the development of efficient mitigation strategy: an integrated system design approach. J. Environ. Chem. Eng. 9, 105277. https://doi.org/10.1016/j.jece.2021.105277.
Bernardo, E., Scarinci, G., Bertuzzi, P., Ercole, P., Ramon, L., 2010. Recycling of waste glasses into partially crystallized glass foams. J. Porous Mater. 17, 359–365. https://doi.org/10.1007/s10934-009-9286-3.
Bish, D.L., Howard, S.A., 1988. Quantitative phase analysis using the Rietveld method. J. Appl. Crystallogr. 21, 86–91. https://doi.org/10.1107/S0021889887009415.
Bish, D.L.L., Post, J.E.E., 1993. Quantitative mineralogical analysis using the Rietveld full-pattern fitting method. Am. Mineral. 78, 932–940.
Bumanis, G., Bajare, D., Locs, J., Korjakins, A., 2013. Alkali-silica reactivity of foam glass granules in structure of lightweight concrete. Construct. Build. Mater. 47, 274–281. https://doi.org/10.1016/j.conbuildmat.2013.05.049.
Buonanno, G., Carotenuto, A., Giovinco, G., Massarotti, N., 2003. Experimental and theoretical modeling of the effective thermal conductivity of rough steel spheroid packed beds. J. Heat Tran. 125, 693–702. https://doi.org/10.1115/1.1578504.
Bush, A.L., Bryan, D.P., Hack, D.R., 2006. Lightweight aggregates. Ind. Miner. rocks Commod. Mark. uses. Metall. Explor. Soc. Min. 37, 181–194. https://doi.org/10.1016/j.clay.2006.11.004.
Cáceres, J.R., Rojas, J.P., Sánchez, J., 2019. A review about the use of industrial by-products in the lightweight aggregates production of expanded clay. In: Journal of Physics: Conference Series. https://doi.org/10.1088/1742-6596/1388/1/012011.
Camana, D., Manzardo, A., Toniolo, S., Gallo, F., Scipioni, A., 2021. Assessing environmental sustainability of local waste management policies in Italy from a circular economy perspective. An overview of existing tools. Sustain. Prod. Consum. 27, 613–629. https://doi.org/10.1016/j.spc.2021.01.029.

Chinnu, S.N., Minnu, S.N., Bahurudeen, A., Senthilkumar, R., 2021. Recycling of industrial and agricultural wastes as alternative coarse aggregates: a step towards cleaner production of concrete. Construct. Build. Mater. 287, 123056. https://doi.org/10.1016/j.conbuildmat.2021.123056.

Collepardi, M., Collepardi, S., Troli, R., 2016. Il Nuovo Calcestruzzo, sixth ed. Enco srl.

Cucciniello, C., Melluso, L., le Roex, A.P., Jourdan, F., Morra, V., de' Gennaro, R., Grifa, C., 2017. From olivine nephelinite, basanite and basalt to peralkaline trachyphonolite and comendite in the Ankaratra volcanic complex, Madagascar: $^{40}Ar/^{39}Ar$ ages, phase compositions and bulk-rock geochemical and isotopic evolution. Lithos 274–275, 363–382. https://doi.org/10.1016/j.lithos.2016.12.026.

de Gennaro, R., Cappelletti, P., Cerri, G., de' Gennaro, M., Dondi, M., Langella, A., 2004. Zeolitic tuffs as raw materials for lightweight aggregates. Appl. Clay Sci. 25, 71–81. https://doi.org/10.1016/j.clay.2003.08.005.

de Gennaro, R., Cappelletti, P., Cerri, G., de' Gennaro, M., Dondi, M., Graziano, S.F.F., Langella, A., 2007. Campanian Ignimbrite as raw material for lightweight aggregates. Appl. Clay Sci. 37, 115–126. https://doi.org/10.1016/j.clay.2006.11.004.

de Gennaro, R., Graziano, S.F., Cappelletti, P., Colella, A., Dondi, M., Langella, A., De'Gennaro, M., 2009. Structural concretes with waste-based lightweight aggregates: from landfill to engineered materials. Environ. Sci. Technol. 43, 7123–7129. https://doi.org/10.1021/es9012257.

Dell'Isola, M., D'Ambrosio Alfano, F.R., Giovinco, G., Ianniello, E., 2012. Experimental analysis of thermal conductivity for building materials depending on moisture content. Int. J. Thermophys. 33, 1674–1685. https://doi.org/10.1007/s10765-012-1215-z.

Dondi, M., Guarini, G., Venturi, I., 2001. Assessing the fusibility of feldspathic fluxes for ceramic tiles by hot stage microscope. Ind. Ceram. 21, 67–73.

Dondi, M., Guarini, G., Raimondo, M., Zanelli, C., 2009. Recycling PC and TV waste glass in clay bricks and roof tiles. Waste Manag. 29, 1945–1951. https://doi.org/10.1016/j.wasman.2008.12.003.

Dondi, M., Cappelletti, P., D'Amore, M., de Gennaro, R., Graziano, S.F., Langella, A., Raimondo, M., Zanelli, C., 2016. Lightweight aggregates from waste materials: reappraisal of expansion behavior and prediction schemes for bloating. Construct. Build. Mater. 127, 394–409. https://doi.org/10.1016/j.conbuildmat.2016.09.111.

Ducman, V., Mladenovič, A., Šuput, J.S., 2002. Lightweight aggregate based on waste glass and its alkali-silica reactivity. Cement Concr. Res. 32, 223–226. https://doi.org/10.1016/S0008-8846(01)00663-9.

Fennis, S.A.A.M., Walraven, J.C., 2012. Using particle packing technology for sustainable concrete mixture design. Heron 57, 73–101.

Fluegel, A., 2007. Glass viscosity calculation based on a global statistical modelling approach. Glas. Technol. Eur. J. Glas. Sci. Technol. Part A 48, 13–30.

Frattolillo, A., Giovinco, G., Mascolo, M.C., Vitale, A., 2005. Effects of hydrophobic treatment on thermophysical properties of lightweight mortars. Exp. Therm. Fluid Sci. 30, 27–35. https://doi.org/10.1016/j.expthermflusci.2004.12.006.

García-Ten, F.J., Quereda Vázquez, M.F., Gil Albalat, C., Chumillas Villalba, D., Zaera, V., Segura Mestre, M.C., 2016. Life ceram-zero waste in ceramic tile manufacture. Key Eng. Mater. 663, 23–33.

Giordano, D., 2019. Advances in the rheology of natural multiphase silicate melts: importance for magma transport and lava flow emplacement. Ann. Geophys. 62, 1–24. https://doi.org/10.4401/ag-7859.

Giordano, D., Russell, J.K., Dingwell, D.B., 2008. Viscosity of magmatic liquids: a model. Earth Planet Sci. Lett. 271, 123–134. https://doi.org/10.1016/j.epsl.2008.03.038.

Hermans, J.M., Peelen, J.G.J., Bei, R., 2001. Recycling of TV glass: profit or doom? Am. Ceram. Soc. Bull. 80, 51–56.

ISO/IEC Guide 98-1, 2009. Uncertainty of Measurement.

Kaz'mina, O.V., 2010. Effect of the component composition and oxidation - reduction characteristics of mixes on foaming of pyroplastic silicate pastes. Glass Ceram. 67, 109–113. https://doi.org/10.1007/s10717-010-9239-y.

Kourti, I., Cheeseman, C.R., 2010. Properties and microstructure of lightweight aggregate produced from lignite coal fly ash and recycled glass. Resour. Conserv. Recycl. 54, 769–775. https://doi.org/10.1016/j.resconrec.2009.12.006.

Kurpińska, M., Ferenc, T., 2020. Experimental and numerical investigation of mechanical properties of light weight concretes (LWCs) with various aggregates. Materials 13, 1–16. https://doi.org/10.3390/MA13163474.

Li, X., He, C., Lv, Y., Jian, S., Jiang, W, Jiang, D., Wu, K., Dan, J., Effect of sintering temperature and dwelling time on the characteristics of lightweight aggregate produced from sewage sludge and waste glass powder. Ceram. Int., https://doi.org/10.1016/j.ceramint.2021.08.250.

Li, X., He, C., Lv, Y., Jian, S., Liu, G., Jiang, W., Jiang, D., 2020. Utilization of municipal sewage sludge and waste glass powder in production of lightweight aggregates. Construct. Build. Mater. 256 https://doi.org/10.1016/j.conbuildmat.2020.119413.

Lim, Y.C., Lin, S.K., Ju, Y.R., Wu, C.H., Lin, Y.L., Chen, C.W., Dong, C.Di, 2019. Reutilization of dredged harbor sediment and steel slag by sintering as lightweight aggregate. Process Saf. Environ. Protect. 126, 287–296. https://doi.org/10.1016/j.psep.2019.04.020.

Liu, R., Coffman, R., 2016. Lightweight aggregate made from dredged material in green roof construction for stormwater management. Materials 9, 1–16. https://doi.org/10.3390/ma9080611.

Lydon, F.D., 1972. Concrete Mix Design. Applied Science Publishers Limited.

Ma, D., Yi, H., Lai, C., Liu, X., Huo, X., An, Z., Li, L., Fu, Y., Li, B., Zhang, M., Qin, L., Liu, S., Yang, L., 2021. Critical review of advanced oxidation processes in organic wastewater treatment. Chemosphere 275, 130104. https://doi.org/10.1016/j.chemosphere.2021.130104.

Méar, F., Yot, P., Cambon, M., Ribes, M., 2006. The characterization of waste cathode-ray tube glass. Waste Manag. 26, 1468–1476. https://doi.org/10.1016/j.wasman.2005.11.017.

Mindness, S., Young, J.F., Darwin, D., 2002. Concrete, second ed. Pearson Prentice Hall.

Molinari, C., Zanelli, C., Guarini, G., Dondi, M., 2020. Bloating mechanism in lightweight aggregates: effect ofprocessing variables and properties of the vitreous phase. Construct. Build. Mater. 261, 119980. https://doi.org/10.1016/j.conbuildmat.2020.119980.

Molinari, C., Zanelli, C., Laghi, L., De Aloysio, G., Santandrea, M., Guarini, G., Conte, S., Dondi, M., 2021. Effect of scale-up on the properties of PCM-impregnated tiles containing glass scraps. Case Stud. Constr. Mater. 14, e00526 https://doi.org/10.1016/j.cscm.2021.e00526.

Monteiro, M.A., Raupp-Pereira, F., Ferreira, V.M., Labrincha, J.A., Dondi, M., 2004. Lightweight aggregates made of industrial wastes or sub-products. Proc. RILEM 2004 Conf. Recycl. Mater. Build. Struct. 1, 107–114.

Moreno-Maroto, J.M., Cobo-Ceacero, C.J., Uceda-Rodríguez, M., Cotes-Palomino, T., Martínez García, C., Alonso-Azcárate, J., 2020. Unraveling the expansion mechanism in lightweight aggregates: demonstrating that bloating barely requires gas. Construct. Build. Mater. 247, 3–5. https://doi.org/10.1016/j.conbuildmat.2020.118583.

Mpatani, F.M., Han, R., Aryee, A.A., Kani, A.N., Li, Z., Qu, L., 2021. Adsorption performance of modified agricultural waste materials for removal of emerging micro-contaminant bisphenol A: a comprehensive review. Sci. Total Environ. 780, 146629. https://doi.org/10.1016/j.scitotenv.2021.146629.

Mueller, A., Sokolova, S.N.N., Vereshagin, V.I.I., 2008. Characteristics of lightweight aggregates from primary and recycled raw materials. Construct. Build. Mater. 22, 703–712. https://doi.org/10.1016/j.conbuildmat.2007.06.009.

Neville, A.M., 2012. Properties of Concrete, fifth ed. Pearson Education Limited.

Oktay, H., Yumrutaş, R., Akpolat, A., 2015. Mechanical and thermophysical properties of lightweight aggregate concretes. Construct. Build. Mater. 96, 217–225. https://doi.org/10.1016/j.conbuildmat.2015.08.015.

Opila, E.J., Nguyen, Q.N., 1998. Oxidation of chemically-vapor-deposited silicon carbide in carbon dioxide. J. Am. Ceram. Soc. 81, 1949–1952.

Pacenti, V., 1980. Il Calcestruzzo Nell'edilizia Moderna. Tecnologia Ed Applicazioni . Dedalo Il Politecnico.

Pascual, A.B., Tognonvi, T.M., Tagnit-Hamou, A., 2021. Optimization study of waste glass powder-based alkali activated materials incorporating metakaolin: activation and curing conditions. J. Clean. Prod. 308 https://doi.org/10.1016/j.jclepro.2021.127435.

Petersen, R.R., König, J., Yue, Y., 2017. The viscosity window of the silicate glass foam production. J. Non-Cryst. Solids 456, 49–54. https://doi.org/10.1016/j.jnoncrysol.2016.10.041.

Proussevitch, A.A., Sahagian, D.L., Kutolin, V.A., 1993. Stability of foams in silicate melts. J. Volcanol. Geoth. Res. 59, 161–178. https://doi.org/10.1016/0377-0273(93)90084-5.

Raimondo, M., Zanelli, C., Matteucci, F., Guarini, G., Dondi, M., Labrincha, J.A., 2007. Effect of waste glass (TV/PC cathodic tube and screen) on technological properties and sintering behaviour of porcelain stoneware tiles. Ceram. Int. 33 (4), 615–623.

Rietveld, H.M., 1969. A profile refinement method for nuclear and magnetic structures. J. Appl. Crystallogr. 2, 65–71.

Samson, G., Phelipot-Mardelé, A., Lanos, C., 2017. A review of thermomechanical properties of lightweight concrete. Mag. Concr. Res. 69, 201–216. https://doi.org/10.1680/jmacr.16.00324.

Sarani, N.A., Kadir, A.A., Rahim, A.S.A., Mohajerani, A., 2018. Properties and environmental impact of the mosaic sludge incorporated into fired clay bricks. Construct. Build. Mater. 183, 300–310.

Tuan, B.L.A.L.A., Hwang, C.-L., Lin, K.-L., Chen, Y.-Y., Young, M.-P., 2013. Development of lightweight aggregate from sewage sludge and waste glass powder for concrete. Construct. Build. Mater. 47, 334–339. https://doi.org/10.1016/j.conbuildmat.2013.05.039.

UNI 11013, European Standard, 2002. Lightweight Aggregates. Expanded Clay and Slate. Assessment of the Properties by Standard Lab Concrete Tests.

UNI EN 12390-1, European Standard, 2012. Testing Hardened Concrete. Part 1: Shape, Dimensions and Other Requirements for Specimen and Moulds.

UNI EN 12390-2, European Standard, 2019. Testing Hardened Concrete. Part 2: Making and Curing Specimen for Strenght Tests.

UNI EN 12390-3, European Standard, 2019. Testing Hardened Concrete. Part 3: Compressive Strength of Test Specimens.

UNI EN 12390-4, European Standard, 2019. Testing Hardened Concrete. Part 4: Compressive Strength - Specifications for Testing Machines.

UNI EN 12390-7, European Standard, 2021. Testing Hardened Concrete. Part 7: Density of Hardened Concrete.

UNI EN 13055, European Standard, 2016. Lightweight Aggregates.

UNI EN 1745, 2020. European Standard Masonry and Masonry Products - Methods for Determining Thermal Properties.

UNI EN 206, European Standard, 2016. Concrete - Specification, Performance, Production and Conformity.

Upadhyay, A., Laing, T., Kumar, V., Dora, M., 2021. Exploring barriers and drivers to the implementation of circular economy practices in the mining industry. Resour. Pol. 72, 102037. https://doi.org/10.1016/j.resourpol.2021.102037.

Wan, K., Huang, L., Yan, J., Ma, B., Huang, X., Luo, Z., Zhang, H., Xiao, T., 2021. Removal of fluoride from industrial wastewater by using different adsorbents: a review. Sci. Total Environ. 773, 145535. https://doi.org/10.1016/j.scitotenv.2021.145535.

Wang, H., Chen, Z., Liu, L., Ji, R., Wang, X., 2018. Synthesis of a foam ceramic based on ceramic tile polishing waste using SiC as foaming agent. Ceram. Int. 44, 10078–10086. https://doi.org/10.1016/j.ceramint.2018.02.211.

Wei, Y.-L., Lin, C.-Y., Ko, K.-W., Wang, H.P., 2011. Preparation of low water-sorption lightweight aggregates from harbor sediment added with waste glass. Mar. Pollut. Bull. 63, 135–140. https://doi.org/10.1016/j.marpolbul.2011.01.037.

Xie, J., Liu, J., Liu, F., Wang, J., Huang, P., 2019. Investigation of a new lightweight green concrete containing sludge ceramsite and recycled fine aggregates. J. Clean. Prod. 235, 1240–1254. https://doi.org/10.1016/j.jclepro.2019.07.012.

Yao, Z., Ling, T.C., Sarker, P.K., Su, W., Liu, J., Wu, W., Tang, J., 2018. Recycling difficult-to-treat e-waste cathode-ray-tube glass as construction and building materials: a critical review. Renew. Sustain. Energy Rev. https://doi.org/10.1016/j.rser.2017.08.027.

Yio, M.H.N., Xiao, Y., Ji, R., Russell, M., Cheeseman, C., 2021. Production of foamed glass-ceramics using furnace bottom ash and glass. Ceram. Int. 47, 8697–8706. https://doi.org/10.1016/j.ceramint.2020.11.103.

Zanelli, C., Conte, S., Molinari, C., Soldati, R., Dondi, M., 2021. Waste recycling in ceramic tiles: a technological outlook. Resour. Conserv. Recycl. 168, 105289. https://doi.org/10.1016/j.resconrec.2020.105289.